Confinement and Interaction of Single Indirect Excitons in a Voltage-Controlled Trap Formed Inside Double InGaAs Quantum Wells

G. J. Schinner,[1] J. Repp,[1] E. Schubert,[1] A. K. Rai,[2] D. Reuter,[2] A. D. Wieck,[2] A. O. Govorov,[1,3] A. W. Holleitner,[4] and J. P. Kotthaus[1]

[1]*Center for NanoScience and Fakultät für Physik, Ludwig-Maximilians-Universität, Geschwister-Scholl-Platz 1, 80539 München, Germany*

[2]*Angewandte Festkörperphysik, Ruhr-Universität Bochum, Universitätsstraße 150, 44780 Bochum, Germany*

[3]*Department of Physics and Astronomy, Ohio University, Athens, Ohio 45701, USA*

[4]*Walter Schottky Institut and Physik-Department, Am Coulombwall 4a, Technische Universität München, D-85748 Garching, Germany*

(Received 4 May 2012; published 19 March 2013)

Voltage-tunable quantum traps confining individual spatially indirect and long-living excitons are realized by providing a coupled double quantum well with nanoscale gates. This enables us to study the transition from confined multiexcitons down to a single, electrostatically trapped indirect exciton. In the few exciton regime, we observe discrete emission lines identified as resulting from a single dipolar exciton, a biexciton, and a triexciton, respectively. Their energetic splitting is well described by Wigner-like molecular structures reflecting the interplay of dipolar interexcitonic repulsion and spatial quantization.

DOI: 10.1103/PhysRevLett.110.127403 PACS numbers: 78.67.De, 71.35.Lk, 72.20.Jv, 78.55.−m

Trapping atoms or ions with tailored electromagnetic fields as on microfabricated chips [1,2] or in optical lattices [3] has enabled detailed studies of quantum systems such as Bose-Einstein condensates [1], coupled ion arrays [2], and atomic Mott insulators [3]. This allowed particle entanglement [1,2] and yielded insight into light matter interactions with individual quantum objects with unprecedented precision. In solid-state devices, similarly, single electron manipulation in charge quantum dots [4–7] or Bose-Einstein condensation (BEC) of two-dimensional bosonic systems in equilibrium both require a trapping potential [8]. So far, optically active quantum dots trapping few excitons rely on three-dimensional material modulation as in self-assembled quantum dots [9–12], providing limited control of confinement potential and position. Here, we demonstrate in tuneable nanoscale traps that tight electrostatic confinement of excitons creates discrete excitonic transitions observable down to a single confined exciton. Such traps combine a double quantum well with gate-defined electrostatic potentials [13]. With their electron and hole confined to a different quantum well, these excitons exhibit a large dipole moment and long lifetimes. Reducing the electrostatic confinement to nanoscale dimensions, we enter the few exciton regime and observe discrete spectral features reflecting interexcitonic dipolar repulsion to cause molecularlike spatial arrangements of two and three excitons, respectively. The excitonic transitions are tuneable by gate voltages and magnetic fields and are well reproduced by a straightforward model. The scheme introduces a new gate-defined platform for creating and controlling single exciton traps and opens the route to lithographically defined arrays of artificial atoms with tuneable in-plane coupling and voltage-controlled optical properties of single charge and spin states. Such arrays may prove useful for scalable, solid-state-based quantum information processing [14–19] and for experimental realizations of various regimes of many-body excitonic states.

In solids, quantum confinement of charge carriers in all three spatial directions results in so-called quantum dots (QD), artificial atoms with discrete energy spectra. Charge quantum dots containing unipolar charges and studied via electronic transport spectroscopy usually utilize electrostatic fields to completely confine charge carriers of a two-dimensional electron system at a heterojunction interface [4,5,7] or in a one-dimensional nanowire [6,7]. In contrast, optically active quantum dots containing both conduction band electrons and valence band holes so far require three-dimensional material modulation by suitable growth methods as in widely studied self-assembled quantum dots [9–12] in order to confine both electrons and holes in the same nanoscale region as bound excitonic pairs; thereby it is difficult to control their position to achieve scalable QD circuits and their confining potential. However, introducing charge tuneability via field effect has enabled us to visualize shell structure of single electron states and precision optical spectroscopy on individual self-assembled quantum dots in emission [11] and absorption [20] and continues to reveal new many-body quantum phenomena [12].

In an effort to combine the advantages of the above approaches, we present a scheme to define optically active quantum traps confining individual indirect dipolar excitons (IX) by electrostatic fields provided via lithographically fabricated nanoscale gates on a suitably designed double quantum well (DQW) heterostructure. By reducing

the trap area and the corresponding IX occupation about 1000-fold in comparison to previous studies [13,21], we achieve the single exciton limit for electrostatically trapped and long-living dipolar excitons. We thus are able to observe discrete emission lines for the single exciton (1IX), biexciton (2IX), and triexciton (3IX) states reflecting quantum dot behavior dominated by the effect of dipolar repulsion between individual excitons, in excellent agreement with a model of interacting IX in a tight parabolic confinement potential. This enables position control of such QDs with lithographic precision as in charge and spin QDs. In addition, it permits electrical tuneability of the excitonic confining potential, photoluminescence (PL) energy and lifetime, and the exciton population down to a single exciton. Based on our approach, one can envision the control of individual excitons in the DQW plane within QDs or in QD arrays with gate-controlled in-plane coupling as needed for implementation in quantum information processing circuits [14–17]. Furthermore, IX are particularly attractive for coherent manipulation because of their long charge and spin lifetimes [22,23].

The three-dimensional confining scheme in the IX quantum traps is based on gate control of the quantum confined Stark effect in the plane of a DQW as illustrated in Fig. 1. The electric field component F_z in the growth direction (z) of the coupled DQW consisting of two adjacent 7 nm wide $In_{0.11}Ga_{0.89}As$ QWs separated by center-to-center distance

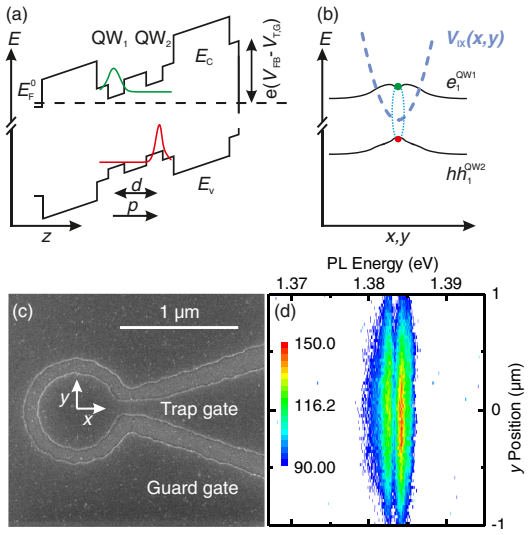

FIG. 1 (color online). (a) Scheme of the DQW band gap within a field-effect device. E_C and E_V denote the conduction and valence band edge, respectively. The electron and hole wave function of the ground states hh_1^{QW2} and e_1^{QW1} are indicated. The energetic tilt of the DQW is tuned by the gate voltages $V_{T,G}$ with respect to the flatband voltage $V_{FB} \sim 0.75$ V. (b) In-plane variation of the hh_1^{QW2} and e_1^{QW1} ground state and the resulting confinement potential V_{IX}. (c) Displays a scanning electron micrograph of the gate pattern. (d) Logarithmically displays the PL intensity vs energy and position y at $x = 0$ [$V_G = 0.75$ V, $V_T = 0.25$ V, $T_{Lattice} = 242$ mK, $P_{Laser} = 2.8n$ W, $E_{Laser} = 1.494$ eV].

of $d = 17$ nm is tuned by a voltage V applied to semitransparent titanium gates with respect to an n-doped GaAs back contact with Fermi energy E_F^0 as shown in the energy diagram in Fig. 1(a). The e-h separation causes a redshift $\Delta E_{IX} = -pF_z$ of the IX energy where $p = ed$ is the IX dipole moment oriented along z. The parabolic confinement V_{IX} in the x-y plane [Fig. 1(b)] is achieved by biasing the trap gate [Fig. 1(c)] with a diameter of 600 nm at a negative voltage V_T with respect to the guard gate. The latter is biased close to the flatband voltage V_{FB} at which the built-in field caused by surface states is canceled by the gate voltage. Coulomb attraction by the hole localized beneath the center of the trap gate binds the electron with a typical binding energy of 3 meV and prevents excitonic ionization by the external in-plane electric field. The spatial separation of the electron and hole along z reduces the overlap of the corresponding wave functions [Fig. 1(a)] resulting in a radiative lifetime of order 100 ns for the IX [24]. Filling the QD with an increasing number of individual IXs allows the investigation of the interplay between dipolar IX-IX repulsion and spatial quantization in the QD. In addition, raising the number of hydrogenlike bosonic IXs, one enters the interesting regime where excitonic BEC is expected, as predicted in the 1960s [25]. Recently, micrometer scale electrostatic trapping configurations were reported to realize a cooled ensemble of indirect excitons with high densities in order to implement a BEC [13,24,26].

The devices are investigated in a low temperature microscope with two diffraction limited confocal objectives that can be independently positioned in a ^{3}He refrigerator at 240 mK. Using the upper objective, we create IXs under the guard gate with laser light 1.2 μm away from the trap center. The quantum trap is thus only filled with IXs precooled to lattice temperatures, whereas free electrons are unable to enter the trap [13]. The emitted PL light is collected in transmission with a second objective located below the device and analyzed in a spectrometer. An image of the PL intensity [Fig. 1(d)] shows two discrete energy-resolved lines emitted from a single exciton and a biexciton (as discussed below) located in the center of the trap. They are spatially diffraction broadened to 900 nm full width at half maximum, comparable to the emitted PL wavelength. The PL of direct excitons occurring in close vicinity of the focus of the exciting laser is discussed in Refs. [13,24].

The population of the QD can be varied by changing the laser power exciting IXs in the vicinity of the QD [Fig. 2(a)]. For excitation laser powers up to 300 pW incident on the sample surface, we observe a single narrow PL line, which we associate with an individual IX. Increasing the laser power generates two discrete PL lines [see also Fig. 1(d)] demonstrating the occupation of the QD with a biexciton decaying via a single IX. A further increase in excitation power creates in addition triexcitons and so on. The discrete PL lines are narrow (~ 0.4 meV) but orders of magnitude broader than expected from the

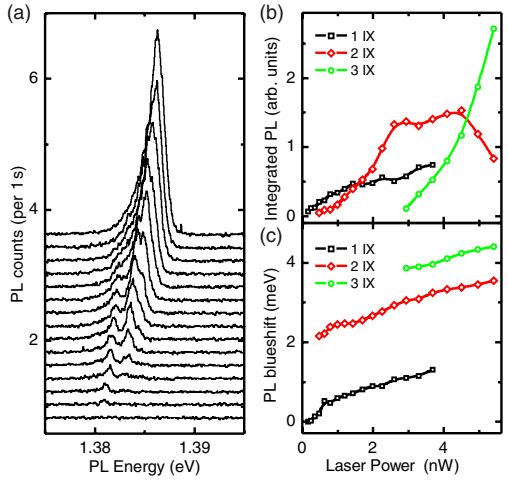

FIG. 2 (color online). (a) PL spectra for different occupations of the trap nonlinearly changed by laser power between 55 pW and 10 nW. In comparison to the emission from individual self-assembled InGaAs quantum dots, PL counts in the single exciton limit are typically found to be 1000-fold lower, reflecting the correspondingly increased radiative lifetime of IX. The corresponding integrated PL intensity and PL blueshift are shown in (b) and (c) [$V_G = 0.65$ V, $V_T = 0.30$ V, $T_{Lattice} = 245$ mK, $E_{Laser} = 1.494$ eV].

radiative lifetime of 300 ns. This we attribute to temporal spectral fluctuations happening during the long integration times of order 200 seconds necessary for detection. The dependence of the PL intensity on the laser power shown in [Fig. 2(b)] is characteristic for a QD populated with multi-excitons [27] rising, e.g., quadratically in laser power for a biexciton. The center energies of the discrete PL lines plotted in Fig. 2(c) reflect the interplay between dipolar interexcitonic repulsion and spatial quantization leading to a splitting of nearly 2 meV between the single exciton and biexciton configuration.

Based on a semiclassical model [24], we can describe the level structure by the following scenario. With the heavy hole fixed in space by the gate-induced electrostatic confining potential, somewhat roughened by the random disorder potential, the light electron in the adjacent QW is electrostatically bound to the hole via Coulomb attraction [Fig. 1(b)]. Filling an additional IX into the narrow lateral confining potential of the QD trap causes strong excitonic repulsion by dipolar interaction. The repulsive energy of about 2 meV at a lateral interexcitonic distance of about 34 nm [24] dominates the energy splitting between the single IX and biexciton. Adding the third exciton yields a somewhat reduced additional repulsion of about 0.7 meV at a distance of 37 nm if we assume a triangular ordering of the excitons in the trap [24]. The strong dipolar interactions between the few excitons in the quantum dot cause spatial order of the excitons [28], in analogy to Wigner-crystal-like states expected in charge quantum dots [29]. This spatial order results in an excitonic Wigner molecule [Figs. 3(a) and 3(b)] and is likely to be assisted by the fact that the external excitonic potential V_{IX} has a significantly larger spatial extent than the excitons confined to Bohr radii. In addition, screening of the bare trap potential V_{IX} by adding dipolar excitons will modify the effective potential landscape. Increasing the laser power increases the time-averaged population of the trap with biexcitons and triexcitons. The resulting dipolar screening causes a blueshift ΔE reflecting the increasing many-body interactions between the IXs and their temporal dynamics [Fig. 2(c)]. A further increase of the laser power causes the QD to sequentially fill up to about 100 IXs [24]. For high populations, we observe an unstructured asymmetric

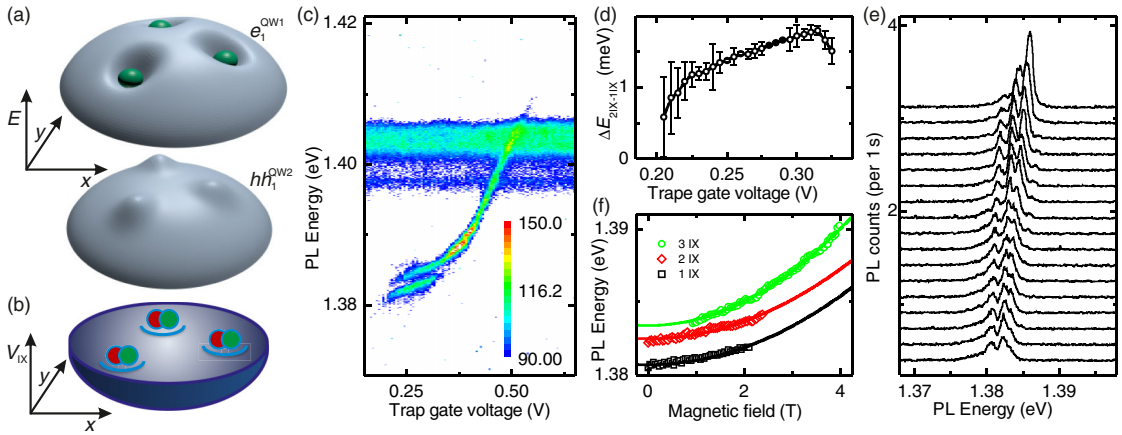

FIG. 3 (color online). (a) Sketches an excitonic Wigner molecule of three equidistantly spaced dipolar excitons confined in parabolic trap potential as displayed in (b). (c) PL energy and intensity (logarithmically plotted) vs trap gate voltage. Below 0.35 V we observe the splitting displayed in (d) [$V_G = 0.55$ V, $T_{Lattice} = 244$ mK, $P_{Laser} = 2.8$ nW, $E_{Laser} = 1.494$ eV]. (e) Characteristic spectra for different magnetic fields in equidistant steps from 0 T (bottom) to 2.5 T (top). From the quadratic fit (solid line) to the PL energies (symbols) in (f) we extract the effective Bohr radii r_e ($r_e^{1IX} = 18.3$ nm, $r_e^{2IX} = 18.4$ nm, and $r_e^{3IX} = 21.7$ nm) [$V_G = 0.75$ V, $V_T = 0.25$ V, $T_{Lattice} = 242$ mK, $P_{Laser} = 2.8$ nW, $E_{Laser} = 1.494$ eV].

PL line shape characterized by a steep blue side and a long red tail [Fig. 2(a)]. The development of the PL line shape in Fig. 2(a) with the trapped exciton density shows clearly that the asymmetric PL line results from the sum of individual exciton PL lines and ends in an edgelike singularity [30,31] for a high density cold dipolar liquid [26,28].

In the quantum trap device, we anticipate to observe correlations because the expected excitonic coherence length [32] exceeds the diameter of the trap, which is also smaller than the emitted PL wavelength. Furthermore, at low temperature (240 mK), the thermal de Broglie wavelength λ_{dB} of the bosonic particles ($\lambda_{\mathrm{dB}} = \frac{\hbar}{\sqrt{2M\pi kT}}$ where $M = m_e^* + m_{\mathrm{hh}}^*$ is the total mass of the exciton) is a few times larger than the interexcitonic distance, which is similar to the effective Bohr radius $r_e \approx 20$ nm.

The excitonic QD potential V_{IX} is tuneable by gate voltage [Fig. 3(c)]. With decreasing trap gate voltage, the trap gets deeper and we expect a narrowing of the lateral confinement down to about 100 nm, inducing a splitting of the PL line in two discrete lines [24]. The latter reflects an occupation of the trap with two exciton states. In Fig. 3(d), the energetic splitting between the exciton and biexciton state is plotted versus the trap gate voltage. We interpret the lowering of the energetic spacing $E_{2\mathrm{IX}} - E_{1\mathrm{IX}}$ with decreasing trap gate voltage by the observation that the time-averaged excitonic population of the quantum trap with biexcitons deduced from the decreasing intensity of the 2 IX PL in Fig. 3(c), and thus the corresponding effective excitonic repulsion weakens and overcompensates the effect of a somewhat increasing electrostatic potential V_{IX}. The splitting is accompanied by a change in the slope of the quantum confined Stark effect [Fig. 3(c)]. Here, we ensured that leakage currents entering the trap gate are negligibly small in the corresponding voltage regime [24]. In traps with a larger trap gate diameter, we are able to observe a gate-voltage-dependent depletion zone of width ranging between 250 nm and 500 nm around the trap perimeter [13,24]. Correspondingly, we expect for the trap depicted in Fig. 1(c) the resulting curvature of the electrostatically induced trap potential V_{IX} to dominate the random disorder potential. Generally, at a trap gate voltage $V_{\mathrm{T}} \gtrsim V_{\mathrm{G}}$, the exciton trap converts into a depopulated antitrap, and we no longer detect any PL from IXs within the trap area.

Additional manifestation of the quantum dot behavior can be deduced from the difference in the diamagnetic energy shifts of the discrete excitonic lines in a magnetic field B applied in Faraday configuration perpendicular to the QW plane. Figure 3(e) displays exemplary PL spectra as a function of B. With increasing magnetic field we observe a diamagnetic shift of the excitonic emission [Fig. 3(f)]. In addition, we observe an increasing PL intensity and the appearance of a triexciton line at higher field. Both findings reflect an increasing magnetic stabilization of excitons. As $B = 0$, a large in-plane component of the electrostatic field near the trap perimeter can cause ionization of the IX. As observed inside QWs [33] and predicted in Ref. [34], such radial tunneling of the excitonically bound electrons out of their pocket in the binding potential [Figs. 1(b) and 3(a)] can be suppressed by a magnetic field along z. For the spectra in Fig. 3(e), this causes both the observed increase in PL intensity and the appearance of a strong triexciton line with increasing B. The resulting quadratic diamagnetic shift of the trapped IXs energies [plotted in Fig. 3(f)] is given by $\Delta E_{\mathrm{dia}} = \frac{e^2 r_e^2}{8\mu c^2} B^2$ where r_e is the effective Bohr radius and μ the reduced mass of the exciton [35]. With increasing exciton number, we see an increase in r_e because the effective confining potential is broadened by screening and strong IX interactions.

In conclusion, we realized individual optically active, gate-defined, and voltage-controlled quantum traps for spatially indirect excitons in which a tuneable potential caused excitonic confinement in the DQW plane. The population of such a QD could be tuned from a single exciton to a multiexciton state of above 100 IXs. With our device, we introduced a gate-defined platform for creating and controlling optically active quantum dots with possible applications in fundamental quantum physics and quantum computing. This provides the possibility of lithographically defined coupled quantum dot arrays with voltage-controlled optical properties and tuneable in-plane coupling.

We thank M. P. Stallhofer, D. Taubert, S. Ludwig, K. Kowalik-Seidl, and A. Högele for stimulating discussions and helpful comments. Financial support by the Deutsche Forschungsgemeinschaft under Project No. Ko 416/17, the SPP1285, as well as the German Excellence Initiative via the Nanosystems Initiative Munich (NIM), LMUexcellent, BMBF QuaHL-Rep (01 BQ 1035), and Volkswagen Foundation are gratefully acknowledged.

[1] M. F. Riedel, P. Böhi, Y. Li, T. W. Hänsch, A. Sinatra, and P. Treutlein, Nature (London) **464**, 1170 (2010).
[2] R. Blatt and D. Wineland, Nature (London) **453**, 1008 (2008).
[3] C. Weitenberg, M. Endres, J. F. Sherson, M. Cheneau, P. Schauß, T. Fukuhara, I. Bloch, and S. Kuhr, Nature (London) **471**, 319 (2011).
[4] R. Hanson, L. P. Kouwenhoven, J. R. Petta, S. Tarucha, and L. M. K. Vandersypen, Rev. Mod. Phys. **79**, 1217 (2007).
[5] A. W. Holleitner, R. H. Blick, A. K. Hüttel, K. Eberl, and J. P. Kotthaus, Science **297**, 70 (2002).
[6] Y. Hu, H. O. H. Churchill, D. J. Reilly, J. Xiang, C. M. Lieber, and C. M. Marcus, Nat. Nanotechnol. **2**, 622 (2007).
[7] S. Hermelin, S. Takada, M. Yamamoto, S. Tarucha, A. D. Wieck, L. Saminadayar, C. Bäuerle, and T. Meunier, Nature (London) **477**, 435 (2011).

[8] P. C. Hohenberg, Phys. Rev. **158**, 383 (1967).
[9] H. Drexler, D. Leonard, W. Hansen, J. P. Kotthaus, and P. M. Petroff, Phys. Rev. Lett. **73**, 2252 (1994).
[10] F. Hatami, M. Grundmann, N. N. Ledentsov, F. Heinrichsdorff, R. Heitz, J. Böhrer, D. Bimberg, S. S. Ruvimov, P. Werner, V. M. Ustinov, P. S. Kop'ev, and Zh. I. Alferov, Phys. Rev. B **57**, 4635 (1998).
[11] R. J. Warburton, C. Schäflein, D. Haft, F. Bickel, A. Lorke, K. Karrai, J. M. Garcia, W. Schoenfeld, and P. M. Petroff, Nature (London) **405**, 926 (2000).
[12] C. Latta, F. Haupt, M. Hanl, A. Weichselbaum, M. Claassen, W. Wuester, P. Fallahi, S. Faelt, L. Glazman, J. von Delft *et al.*, Nature (London) **474**, 627 (2011).
[13] G. J. Schinner, E. Schubert, M. P. Stallhofer, J. P. Kotthaus, D. Schuh, A. K. Rai, D. Reuter, A. D. Wieck, and A. O. Govorov, Phys. Rev. B **83**, 165308 (2011).
[14] D. Loss and D. P. DiVincenzo, Phys. Rev. A **57**, 120 (1998).
[15] A. Imamoglu, D. D. Awschalom, G. Burkard, D. P. DiVincenzo, D. Loss, M. Sherwin, and A. Small, Phys. Rev. Lett. **83**, 4204 (1999).
[16] G. Burkard, D. Loss, and D. P. DiVincenzo, Phys. Rev. B **59**, 2070 (1999).
[17] X. Li, Y. Wu, D. Steel, D. Gammon, T. H. Stievater, D. S. Katzer, D. Park, C. Piermarocchi, and L. J. Sham, Science **301**, 809 (2003).
[18] K. De Greve, L. Yu, P. L. McMahon, J. S. Pele, C. M. Natarajan, N. Y. Kim, E. Abe, S. Maier, C. Schneider, M. Kamp, S. Hofling, R. H. Hadfield, A. Forchel, M. M. Fejer, and Y. Yamamoto, Nature (London) **491**, 421 (2012).
[19] W. B. Gao, P. Fallahi, J. Miguel-Sanchez, and A. Immamoglu, Nature (London) **491**, 426 (2012).
[20] A. Högele, S. Seidl, M. Kroner, K. Karrai, R. J. Warburton, B. D. Gerardot, and P. M. Petroff, Phys. Rev. Lett. **93**, 217401 (2004).
[21] A. A. High, A. T. Hammack, L. V. Butov, L. Mouchliadis, A. L. Ivanov, M. Hanson, and A. C. Gossard, Nano Lett. **9**, 2094 (2009).
[22] Z. Vörös, D. W. Snoke, L. Pfeiffer, and K. West, Phys. Rev. Lett. **103**, 016403 (2009).
[23] K. Kowalik-Seidl, X. P. Vögele, B. N. Rimpfl, S. Manus, J. P. Kotthaus, D. Schuh, W. Wegscheider, and A. W. Holleitner, Appl. Phys. Lett. **97**, 011104 (2010).
[24] See Supplemental Material at http://link.aps.org/supplemental/10.1103/PhysRevLett.110.127403 for confinement potential of circular traps, modeling the energy spectra in a few-exciton trap, lifetime of trapped indirect excitons, temperature dependence, and leakage currents.
[25] J. M. Blatt, K. W. Böer, and W. Brandt, Phys. Rev. **126**, 1691 (1962).
[26] G. J. Schinner, J. Repp, E. Schubert, A. K. Rai, D. Reuter, A. D. Wieck, A. O. Govorov, A. W. Holleitner, and J. P. Kotthaus, arXiv:1111.7175.
[27] K. Brunner, G. Abstreiter, G. Böhm, G. Tränkle, and G. Weimann, Phys. Rev. Lett. **73**, 1138 (1994).
[28] B. Laikhtman and R. Rapaport, Phys. Rev. B **80**, 195313 (2009).
[29] V. M. Bedanov and F. M. Peeters, Phys. Rev. B **49**, 2667 (1994).
[30] M. S. Skolnick, J. M. Rorison, K. J. Nash, D. J. Mowbray, P. R. Tapster, S. J. Bass, and A. D. Pitt, Phys. Rev. Lett. **58**, 2130 (1987).
[31] P. Hawrylak, Phys. Rev. B **44**, 3821 (1991).
[32] S. Yang, A. T. Hammack, M. M. Fogler, L. V. Butov, and A. C. Gossard, Phys. Rev. Lett. **97**, 187402 (2006).
[33] S. Zimmermann, A. O. Govorov, W. Hansen, J. P. Kotthaus, M. Bichler, and W. Wegscheider, Phys. Rev. B **56**, 13414 (1997).
[34] A. O. Govorov and W. Hansen, Phys. Rev. B **58**, 12980 (1998).
[35] M. Stern, V. Garmider, V. Umansky, and I. Bar-Joseph, Phys. Rev. Lett. **100**, 256402 (2008).